WELDING AND WELD REPAIR OF SINGLE CRYSTAL GAS TURBINE ALLOYS

J. M. Vitek, S. A. David, and S. S. Babu

Oak Ridge National Laboratory
P. O. Box 2008
Oak Ridge, TN 37831-6096

ABSTRACT

The cost-effective commercial use of single crystal nickel-based superalloys for land-based turbine engine components such as blades and vanes requires that they can be repair welded to improve as-cast yields or to refurbish worn or failed components after intermediate service intervals. This program addresses this vital need by determining the welding behavior and weldability of single crystal nickel-based superalloys in order to develop an understanding and methodology for weld repair of critical components in advanced gas turbine systems. When welding single crystals, the formation of new grains (stray grains) during solidification must be avoided in order to maintain the single crystal nature of the base material. Preservation of the single crystal microstructure is desired in order to achieve the excellent high temperature creep properties of nickel-based superalloys that are needed in gas turbine applications. In the last year, the primary focus of the project has been on stray-grain formation. The mechanism of stray-grain formation has been evaluated. In addition, modeling has been carried out to identify the optimum welding conditions to avoid stray grains. This was done by combining thermal models, geometric dendritic growth models, and models for the nucleation and growth of stray grains. Preliminary work has also been carried out to identify potential alloy modifications that would minimize stray-grain formation tendencies. This latter work is based on computational thermodynamic modeling of alloy composition variations. The program is coordinated with an industry-university consortium that provides in-kind support and direction to the program.

INTRODUCTION

In order to achieve performance goals for gas turbine engines, high-temperature operation is required. At such high temperatures, creep of structural components must be kept to a minimum and for many metallic components, adequate creep properties can only be achieved with the use of single crystals (see Figure 1). Such single crystals are routinely used in aircraft turbine engines. However, due to the increase in size of land-based turbine engines compared to comparable aircraft turbine engines, component cost will be increased dramatically and component quality will be a major manufacturing concern. In order to take advantage of the potential for high temperature service operation and corresponding improved efficiency afforded by single crystal components, costs must be kept under control. A key factor in reducing costs is the availability of a repair technology that can be used to repair as-cast defects, thereby improving casting yields, and to repair worn or damaged parts.

Earlier work at ORNL has shown that it is possible to weld polycrystalline nickel-based superalloys under limited conditions using electron or laser beam welding (2). However, routine commercial welding of single crystal nickel-based superalloys has three major hurdles that need to be addressed in order to make refurbishment and repair feasible. First, the single crystal nature of the nickel-based superalloys is easily lost during welding due to stray-grain formation (3). Second, nickel-based superalloys are very prone to

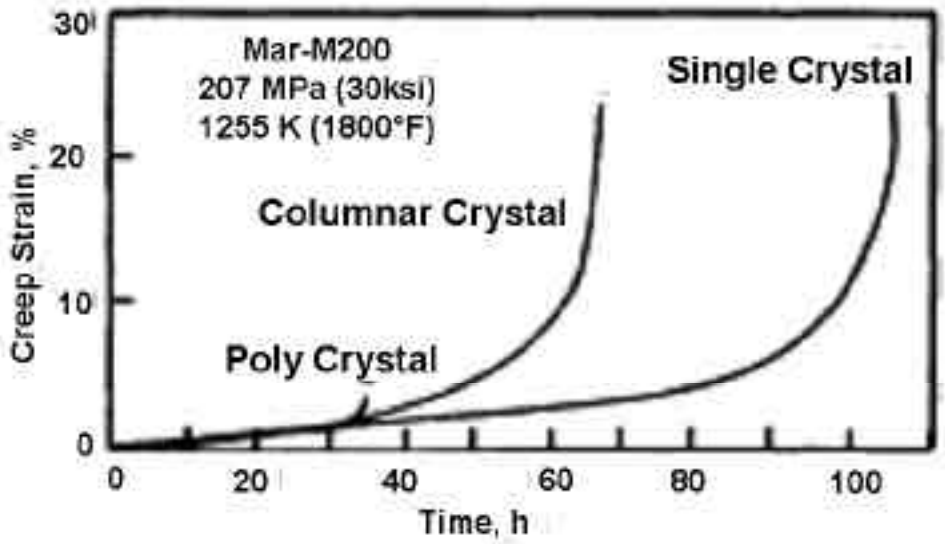

Figure 1: Comparison of creep strain versus time for equiaxed, directionally solidified and single crystal microstructures (from ref 1). Single crystals provide superior performance in creep.

cracking during welding, and the presence of stray grains provides high-angle grain boundaries that act as preferred paths for crack propagation. Finally, non-equilibrium solidification, elemental partitioning, and subsequent solid state transformation can yield microstructures that are not ideal and will not produce material with the needed properties (4,5). In addition to fusion welding, there is a need for the surface buildup of worn components through arc, electron-beam, or laser-beam deposition processes. For such surface deposition, published work by Gäumann et al (6) has shown that the conditions that favor epitaxial growth versus nucleation and growth are related to the temperature gradients, solidification velocities and heat-treatment processes.

The three major hurdles for welding of single-crystal nickel superalloys (stray-grain formation, cracking, and non-equilibrium microstructure formation) are interdependent. It is the objective of this proposal to investigate the potential for weld refurbishment and repair of components by concentrating on these three effects and to determine processes, process conditions, and alloy compositions that will make such weld processing possible. In this year of the project, stray-grain formation, and the means for avoiding it, was examined.

DISCUSSION OF CURRENT ACTIVITIES

MECHANISM OF STRAY-GRAIN FORMATION

Two mechanisms have been proposed to describe stray-grain formation. One considers the fragmentation of growing dendrites due to vigorous fluid flow in the molten pool (7), as shown schematically in the top of Figure 2. The other is based on constitutional supercooling ahead of the advancing dendrite front, leading to nucleation and growth of new grains (8), shown schematically in the bottom of Figure 2. Earlier work in this project has identified several characteristics of stray-grain formation in nickel-based

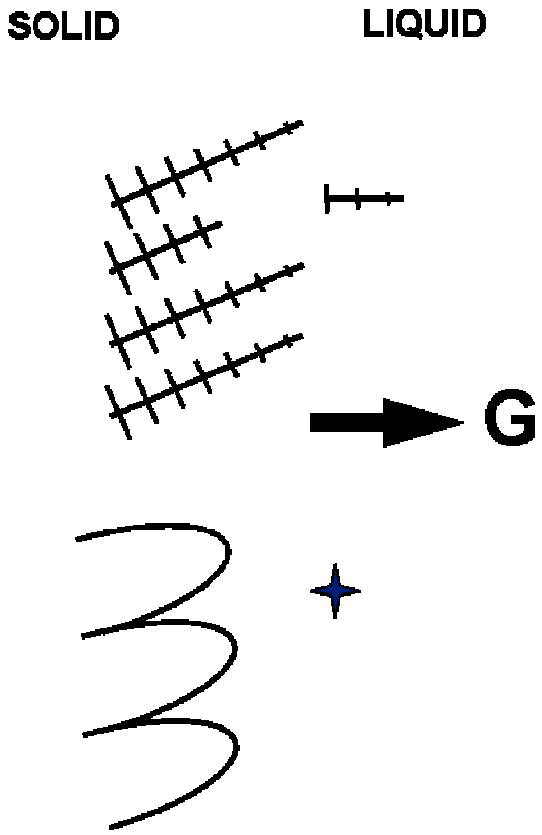

Figure 2: Schematic diagram showing the two possible mechanisms for stray-grain formation. Solidification is from left to right. In the fragmentation mechanism (top), dendrite tips may break off and act as new solidification sites. In the constitutional supercooling mechanism (bottom), new grains may form ahead of the advancing front in the supercooled liquid. In both mechanisms, new grains form most easily when the advancing solidification front is poorly aligned with the thermal gradient (large arrow), as shown in the diagram.

superalloy welds. These are summarized in Table 1, along with indications as to how well the two proposed mechanisms agree with the experimental results. Several of the experimental observations do not agree with predictions based on the fragmentation mechanism. Fragmentation theory predicts that stray-grain formation will be greater at the fusion line, where the cooling rates are highest (7). In addition, to a first order, fragmentation should be symmetrical with respect to the weld centerline, since fluid flow of the melt during welding is basically symmetrical. With further development of the theory, a dependence of fragmentation on orientation may evolve, but at present a dependence that would explain the observed asymmetry does not exist. Fragmentation theory is not developed enough to agree or disagree with other observations. Thus, while fragmentation appears to apply for stray-grain formation in casting, it may only be of secondary importance in welding. This is not unexpected, since the thermal conditions and fluid flow behavior are very different in welding and casting.

The constitutional supercooling mechanism for stray-grain formation has been examined quite extensively in recent years (9-11). It is based on the solute partitioning that takes place during solidification. Rejection of solute ahead of the advancing solidification front leads to a zone of enriched liquid with a suppressed liquidus temperature compared to the overall alloy composition. If the thermal gradient is small, this liquid will be undercooled and nucleation and growth of new grains will be promoted. A simplified treatment of constitutional supercooling leads to the following condition for avoiding supercooling:

$$\frac{G}{V} > \frac{\Delta T}{D} \qquad (1)$$

Table 1: Experimentally observed characteristics of stray-grain formation in welds on commercial alloy Rene N5 and agreement (✓) or disagreement (×) with two potential mechanisms.		
Observation	Fragmentation Theory	Constitutional Supercooling Theory
Stray grains near centerline, not at edge	×	✓
Stray grains can be asymmetrically distributed with respect to the centerline	×	✓
Stray-grain formation varies with weld conditions	No theory	✓
Stray-grain formation varies with composition	No theory	✓

where G is the thermal gradient, V is the growth velocity, _T is the solidification temperature range, and D is the diffusion coefficient in the liquid (8). More advanced treatments have been developed recently and provide a more quantitative assessment of the extent of stray-grain formation (9-11). While many assumptions are included in the theoretical treatment of constitutional supercooling when applied to multi-component systems, such as the Rene N5 alloy used in this study, the theory leads to several specific predictions. With a detailed treatment of the nucleation of new grains, and their growth ahead of the advancing dendritic front, the following relationship was derived (11):

$$\frac{G^n}{V} = a\left[\sqrt[3]{\frac{-4\pi N_0}{3\ln[1-\Phi]}}\,\frac{1}{n+1}\right]^n \qquad (2)$$

where a and n are material constants, N_0 is the nucleation density, and _ is the volume fraction of new, equiaxed grains (i.e, stray grains). A high value of _ ($0.5 < \_ < 1.0$) corresponds to basically complete stray-grain formation, while a small value of _ ($\_ \sim 0$) corresponds to no stray-grain formation. In the present analysis, the values for the three constants ($a = 1.25 \times 10^6$ $sK^{3.4}m^{-1}$, $n = 3.4$, and $N_0 = 2 \times 10^{15}$ m^{-3}) were the same as those used by Gäumann et al (11) for a similar nickel-based superalloy. One can rearrange Equation (2) to solve explicitly for the stray-grain fraction, obtaining:

$$\Phi = 1 - e^S \quad \text{where } S = \frac{-4\pi N_0}{3}\left[\frac{1}{(n+1)(G^n/aV)^{1/n}}\right]^3 = -2.56\times10^{19}\left[\frac{V}{G^{3.4}}\right]^{3/3.4} \qquad (3)$$

In the present analysis, the gradient and solidification front velocity vary across the weld pool. In addition, one must take into account the crystallographic orientation of the single crystal. In FCC materials such as the Rene N5 superalloy, there are six possible variants of the preferred dendritic growth directions ([100], [-100], [010], etc). Growth along any one of these base-metal directions would result in preservation of the single-crystal nature of the sample. At any given location, one must consider the thermal gradient and growth velocity along the six <100> variants. The active dendrite growth direction at any given location is the one corresponding to the minimum growth velocity, which corresponds to the minimum dendrite-tip undercooling (12). When such an analysis was performed, the results were found to be perfectly consistent with the experimental findings. It was found that _ was a minimum at the weld fusion line and increased as the weld centerline was approached, in agreement with the experimental results that showed stray grains near the centerline (Table 1). Taking into account the actual weld sample crystallographic orientation, it was found that _ was asymmetrical with respect to the weld centerline, also

in agreement with the characteristics listed in Table 1. Moreover, the side where stray-grain formation was predicted to be more extensive was the same as that found in experiments. Finally, the calculations showed the formation of stray grains should be greatest in the high power welds at nearly all speeds, also in agreement with experiment. The compositional dependence of stray-grain formation as predicted by constitutional supercooling also agreed with experimental observations; this is described in detail later. Based on these results, it was concluded that the constitutional supercooling mechanism correctly describes stray-grain formation tendencies in welds. This analysis was then used to evaluate the effect of weld conditions on stray-grain formation, as described in detail in the next section.

OPTIMIZATION OF WELDING CONDITIONS TO AVOID STRAY-GRAIN FORMATION

Equation (3) was used to evaluate _ as a function of weld speed, weld power, and weld sample crystallographic orientation. A simple 3D Rosenthal solution was used to describe the shape of the weld pool as a function of speed and power (13). While more accurate models for calculating the weld pool shape are available, the simple solution was used because it allowed for an easy evaluation of the entire weld pool surface, due to the inherent symmetry of the solution. Its simplicity made the calculations less demanding in terms of computational power, so that a wide range of conditions could be studied. Two different analyses were made. In the first, an overall average value of _ ($\__{AV}$) was determined by taking the area-weighted average of _ over the entire weld pool. In the second, the variation of _ as a function of position in the weld pool was examined. Representative results for $\__{AV}$ are presented in Figure 3. $\__{AV}$ is plotted versus weld speed for a single orientation and three weld powers.

The results in Figure 3 show that $\__{AV}$ decreases as the weld speed increases. This was found to be true in general, with only a few exceptions. At first this result appears to violate the simple analysis of constitutional supercooling, as expressed in Equation (1). In that equation, if all other variables are held constant (G, _T, D), then increasing velocity leads to a failure of the condition that must be met to avoid stray-grain formation. However, as the velocity increases, the gradient also increases. A steep gradient helps to avoid stray grains, as described in Equation (1). In fact, the more detailed expressions shown in Equations (2) and (3) show that changes in gradient are far more important than changes in velocity, since the gradient is raised to the 3.4 power.

An overall map of $\__{AV}$ versus weld speed and power is shown in Figure 4. Contour lines have been fitted to the calculated conditions, representing over 20 different combinations of weld speed and power, covering the range of speeds from 0.0042 to 0.42 m/s and powers from 420 to 4000 W. The map in Figure 4 clearly identifies the preferred operating conditions. Low values of $\__{AV}$, corresponding to minimal tendencies to form stray grains during welding, are found at low powers and high weld speeds.

In the second type of analysis, _ was calculated as a function of position in the weld pool. In this analysis, the local variation in thermal conditions and growth velocity are demonstrated, after taking into account the different possible dendrite growth orientations. A typical result is shown in Figure 5 for a weld made at relatively low power and low speed, but made in an asymmetrical orientation ([310] direction on (1 -3 7) plane). The values of _ at any given location are the color coded data points in the figure. Blue represents _ = 0 and red corresponds to _ = 1. Values between 0 and 1 correspond to colors between blue and red. The figure shows many interesting features. The asymmetry in the distribution of _ around the weld pool is clearly seen. In this figure, one side of the weld pool maintains relatively low values of _ throughout, while the other side has a large zone with high values of _ (large zone of nearly pure-red points). It is clearly seen that _ is small at the edge of the weld pool and tends to increase near the centerline. The model results are in perfect agreement with the experimental observations and thereby

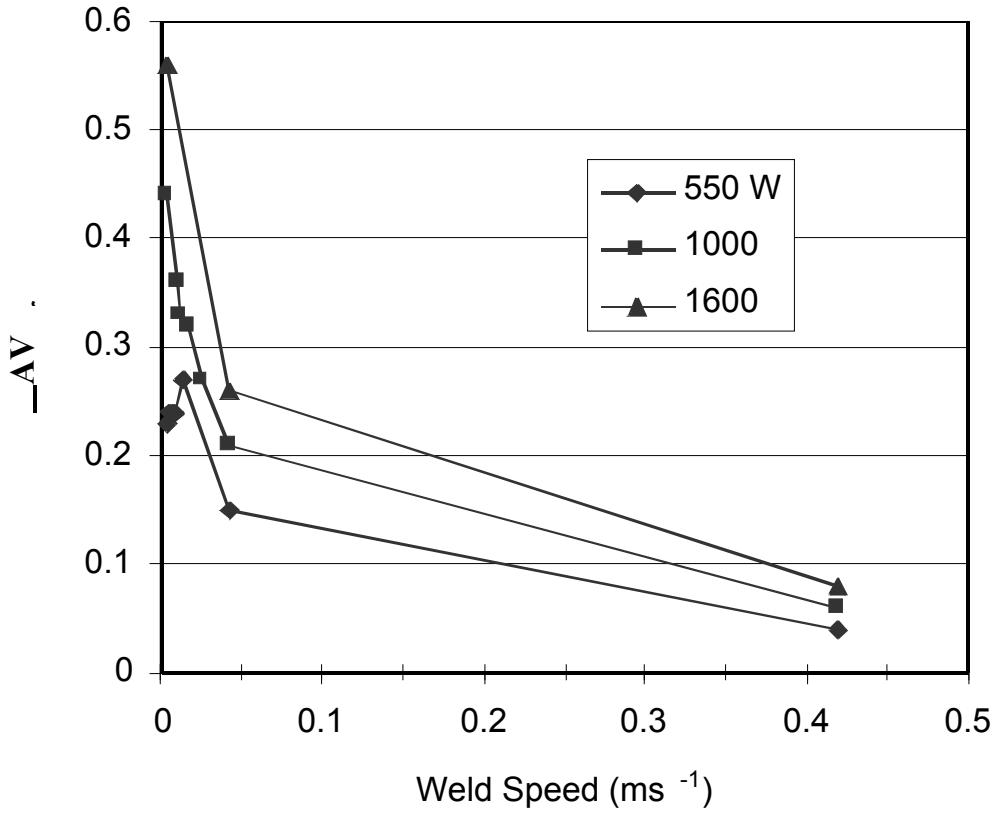

Figure 4: Calculated fraction of stray grains averaged over entire weld pool (η_{AV}) versus weld speed for three fixed weld powers.

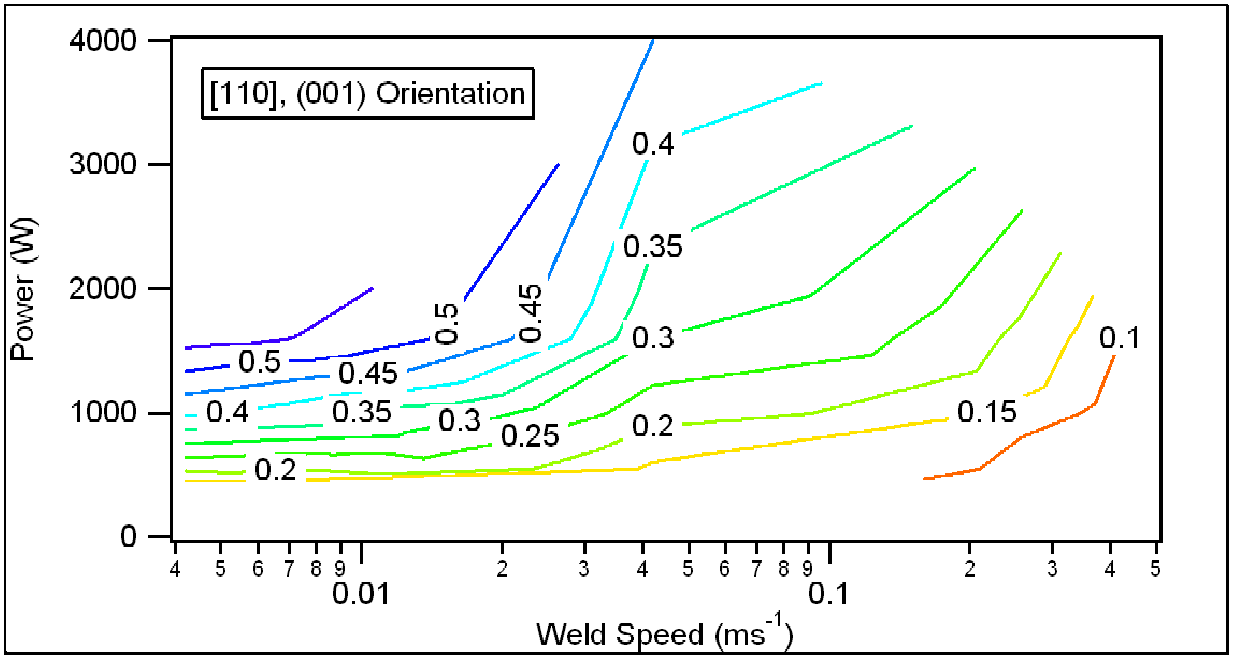

Figure 3: Contour plot of η_{AV} versus weld power and speed for a given weld orientation. High weld speed and low weld power lead to lowest values of η_{AV} .

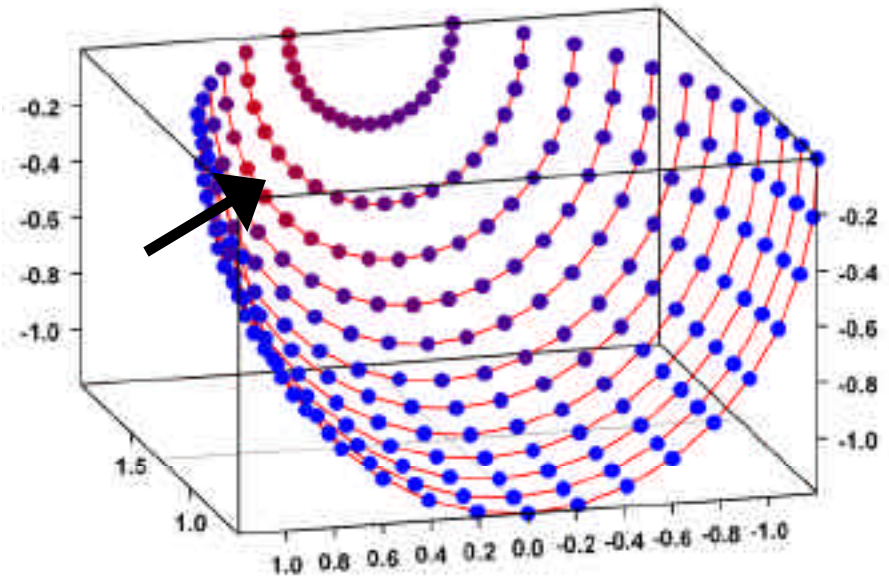

Figure 5: Three-dimensional plot showing local values of _ as a function of position on the weld pool surface. Blue represents _ = 0 (no stray grains) and red represents _ = 1 (all stray grains). The arrow points to the high-_ region, and the asymmetrical behavior of _ in this asymmetrical weld orientation is clear.

support the conclusion that stray-grain formation is described by constitutional supercooling and, moreover, the models reproduce the observed experimental results.

FILLER METAL ALLOY DEVELOPMENT

Preliminary work has been started to identify modifications to commercial alloy compositions that may lead to improved resistance to stray-grain formation. As seen in Equation (1), the solidification temperature range, _T, has a direct impact on the extent of constitutional supercooling. This behavior was confirmed qualitatively by comparing the stray-grain formation tendencies in several alloys, including model alloys. The solidification temperature ranges were calculated by computational thermodynamics (CT) and the results are presented in Table 2. It is seen that as _T increases, the degree of stray-grain formation also increases. Thus, an effort was undertaken to modify the commercial alloy compositions in order to reduce the _T. This was done in two ways. Solidification temperature ranges for many alloy compositions were calculated by CT and the results were used to train a neural network to predict _T as a function of composition. This was used, in turn, to identify an optimum composition. The second approach was to use CT to calculate directly the _T for an extensive matrix of alloy compositions (over 1000 variations). Both approaches identified potential filler metal alloy compositions and efforts are underway to evaluate these alloys.

Table 2: Tendency to form stray grains for different alloys, based on experimental results.

Alloy	Calculated _T	Stray-grain Formation
Pure Fe-15Cr-15Ni	~ 10°C	No stray grains
Less pure Fe-15Cr-15Ni with 1% fourth constituent	~ 20°C	Few stray grains
Commercial Ni superalloys	> 40°C	Many stray grains

REFERENCES

(1) M.J. Donachie and S.J. Donachie in Superalloys, A Technical Guide, ed 2, ASM-International, Materials Park,Ohio, 2002.

(2) S. A. David, J. M. Vitek, S. S. Babu, L. Boatner, and R. W. Reed, "Welding of Nickel-Base Superalloy Single Crystals," *Sci. Technol. Welding and Joining*, Vol. 2, 1997, pp. 79 - 88.

(3) J. M. Vitek, S. A. David, and L. A. Boatner, "Microstructural Development in Single Crystal Nickel-Base Superalloy Welds," *Sci.. Technol. Welding and Joining*, Vol. 2, 1997, pp. 109 - 118.

(4) S. S. Babu, S. A. David, and M. K. Miller, "Microstructural Development in PWA 1480 Electron Beam Welds – An Atom-Probe Filed-Ion Microscope Study," *Applied Surface Science*, Vol. 94/95, 1996, pp. 280 - 287.

(5) S. S. Babu, S. A. David, J. M. Vitek, and M. K. Miller, "Atom-Probe Field Ion Microscopy Investigation of CMSX-4 Ni-Base Superalloy Laser Beam Welds," *J. de Physique IV*, Vol. 6, 1996, pp. C5-253 - 258.

(6) M. Gaumann, S. Henry, F. Cleton, J.-D. Wagniere, and W. Kurz, "Epitaxial Laser Metal Forming: Analysis of Microstructure Formation," *Mat. Sci. Eng*., Vol. A271, 1999, pp. 232 - 241.

(7) T. M. Pollock and W. H. Murphy, "The Breakdown of Single-Crystal Solidification in High Refractory Nickel-Base Alloys," *Metall Mater Trans A*, Vol. 27A, 1996, pp. 1081-1094.

(8) W. Kurz and D. J. Fisher, p 240 in Fundamentals of Solidification, Trans Tech Publications, Aedermannsdorf, Switzerland, 1984.

(9) J. D. Hunt, "Steady State Columnar and Equiaxed Growth of Dendrites and Eutectics", *Mater Sci Eng*, Vol. 65, 1984, pp. 75-83.

(10) M. Gäumann, R. Trivedi and W. Kurz, "Nucleation Ahead of the Advancing Interface in Directional Solidification," *Mater Sci Eng*, Vol. A226-228, 1997, pp. 763-769.

(11) M. Gäumann, C. Bezençon, P. Canalis and W. Kurz, "Single-Crystal Laser Deposition of Superalloys: Processing-Microstructure Maps", *Acta Mater*, Vol. 49, 2001, pp. 1051-1062.

(12) M. Rappaz, S.A. David, J.M. Vitek, and L.A. Boatner, "Analysis of Solidification Microstructures in Fe-Ni-Cr Single Crystal Welds," *Metall. Trans. A*, Vol. 21A, 1990, pp. 1767 – 1782.

(13) D. Rosenthal, "Mathematical Theory of Heat Distribution during Cutting and Welding," *Weld J*, Vol. 20(5), 1941, pp. 220s-234s.